

Uptake of Gaseous Alkylamides by Suspended Sulfuric Acid Particles: Formation of Ammonium/Aminium Salts

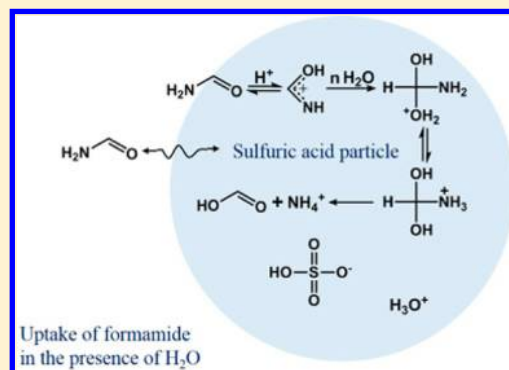
Hangfei Chen,[†] Mingyi Wang,^{†,§} Lei Yao,[†] Jianmin Chen,^{†,‡} and Lin Wang^{*,†,‡}

[†]Shanghai Key Laboratory of Atmospheric Particle Pollution and Prevention (LAP³), Department of Environmental Science & Engineering, Fudan University, Shanghai 200433, China

[‡]Institute of Atmospheric Sciences, Fudan University, Shanghai 200433, China

S Supporting Information

ABSTRACT: Amides represent an important class of nitrogen-containing compounds in the atmosphere that can in theory interact with atmospheric acidic particles and contribute to secondary aerosol formation. In this study, uptake coefficients (γ) of six alkylamides (C_1 to C_3) by suspended sulfuric acid particles were measured using an aerosol flow tube coupled to a high resolution time-of-flight chemical ionization mass spectrometer (HRTof-CIMS). At 293 K and < 3% relative humidity (RH), the measured uptake coefficients for six alkylamides were in the range of $(4.8\text{--}23) \times 10^{-2}$. A negative dependence upon RH was observed for both *N*-methylformamide and *N,N*-dimethylformamide, likely due to decreased mass accommodation coefficients (α) at lower acidities. A negative temperature dependence was observed for *N,N*-dimethylformamide under < 3% RH, also consistent with the mass accommodation-controlled uptake processes. Chemical analysis of reacted sulfuric acid particles indicates that alkylamides hydrolyzed in the presence of water molecules to form ammonium or aminium. Our results suggest that multiphase uptake of amides will contribute to growth of atmospheric acidic particles and alter their chemical composition.



1. INTRODUCTION

Amides refer to a category of nitrogen-containing organic compounds with a general formula of $R_1C(O)NR_2R_3$ (R_1 , R_2 , and R_3 = a hydrogen atom or an alkyl group). They are directly emitted from various sources, including biomass burning,¹ cooking,¹ combustion,² animal husbandry,³ sewage treatment,⁴ and industrial manufacture processes of lubricants, inks, and many other products.⁵ In addition to the primary emission sources, amides can be generated in situ in the atmosphere as well. For example, amides are products formed from the gas-phase reactions of amines with OH and NO₃ radicals and ozone,^{6–9} and from OH radical-initiated reactions of 2-aminoethanol.^{10,11} Amides can also be formed via atmospheric accretion reactions of organic acids with amines or ammonia.¹² In addition, reactions of particulate amines with stabilized Criegee intermediates or secondary ozonides will lead to the formation of amides.¹³

Gaseous amides have been detected close to their sources. Leach et al. measured over 4000 pptv (parts per trillion by volume) of dimethylformamide (DMF) near waste and sewage operations.⁴ Large emissions (4.21 g kg^{-1}) of acetamide (AA) were detected from peat fires burning.¹⁴ Formamide (FA) was detected as a degradation product of 2-aminoethanol emitted from an industrial carbon capture facility.¹⁵ In addition to measurements of amides near the emission sources, Yao et al. recently reported the detection of C_1 - to C_6 -amides in the urban atmosphere of Shanghai using a high resolution time-of-

flight chemical ionization mass spectrometer (HRTof-CIMS):¹⁶ up to hundreds of pptv of amides, and even peak concentrations of 8700 pptv for C_3 -amides, were observed in urban Shanghai.

The detection of high concentrations of amides in the ambient air urges a complete understanding on their atmospheric transformation. Previous studies reported that amides can undergo reactions with atmospheric oxidants including OH and NO₃ radicals, O₃, and Cl atoms,^{5,17–20} leading to nitrogen-containing products that can contribute to the formation of secondary aerosols.^{20–22} On the other hand, acetamide was found to only have a very weak enhancement capability on sulfuric acid nucleation.²³ Nevertheless, amides are expected to interact with acids since they are prone to accept protons. Indeed, previous studies suggest that amides would hydrolyze via the A_O^T2 (acid-catalyzed, oxygen-protonated, tetrahedral intermediate and bimolecular) mechanism in acidic media in the presence of water molecules, giving rise to the formation of ammonium or aminium.^{24,25} Therefore, amides likely interact with atmospheric acidic particles, especially newly formed sulfuric acid particles with a high acidity, and alter their physicochemical properties.

Received: June 21, 2017

Revised: September 6, 2017

Accepted: September 14, 2017

Published: September 14, 2017

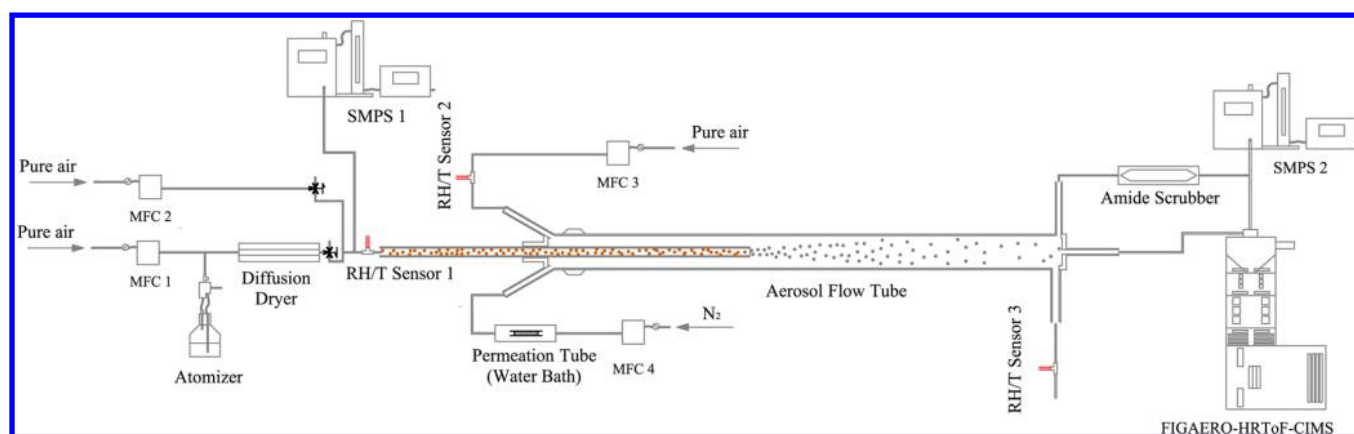


Figure 1. Schematic diagram of the aerosol flow tube system.

In this study, we investigated uptake of six alkylamides by suspended sulfuric acid particles in an aerosol flow tube coupled to a HRTof-CIMS using protonated ethanol reagent ions. The influences of temperature (293–355 K) and relative humidity (<3–80% RH) on uptake coefficients were studied as well to elucidate the rate-determining step during the uptake processes. In addition to kinetic measurements, we analyzed the chemical composition of sulfuric acid particles exposed to FA or DMF at different RH to elucidate the detailed reaction pathway. Atmospheric implications of our study are discussed.

2. MATERIALS AND METHODS

The experimental system for the uptake measurements is illustrated schematically in Figure 1. The aerosol flow tube is made of Pyrex glass with an inner diameter of 8 cm and a total length of 1.2 m. The inlet of the flow tube is characterized with two side-injectors for introduction of gases, and a stainless-steel injector of 8 mm inner diameter that is situated along the tube's centerline for introduction of aerosols. The outlet of the flow tube is connected to online instruments to monitor the progress of uptake experiments. Temperature and RH were monitored using RH/temperature probes (model HMP110, Vaisala Inc., Finland). The majority of experiments were performed at room temperature (293 K). However, there were a set of experiments during which temperatures were regulated between 293 and 355 K by heating the aerosol flow tube with a heating tape.

In this study, a flow of pure air generated by a pure air generator (model 737, AADCO Instruments Inc.) at 2.7 slpm (standard liters per minute) was passed through a commercial constant output atomizer (TSI 3076) that was filled with a diluted H_2SO_4 solution to produce suspended sulfuric acid particles. The outflow was then directed to multiple silica gel dryers to reduce the RH to less than 3%. In case of experiments at a high RH, the aerosol flow was then mixed with a 100% RH pure air flow at different ratios to obtain the desired RH. Subsequently, the aerosol flow was introduced into the aerosol flow tube through the stainless-steel injector. The size distributions of suspended H_2SO_4 particles were measured using two sets of scanning mobility particle sizer (SMPS, consisting of one TSI model 3081 Long DMA and one TSI model 3776 condensation particle counter for both sets) placed before and behind the aerosol flow tube, respectively. A scan over the mobility diameter in the range of 14–700 nm provided a size distribution, from which the total aerosol surface area-to-volume ratio was calculated assuming particles are spherical.

These distributions during the kinetic experiments typically had a geometric standard deviation of 1.5–2.0, with a mean geometric diameter of ~ 100 nm. Aerosol surface area-to-volume ratio was varied over the range of 1×10^9 to 1×10^{11} $\text{nm}^2 \text{cm}^{-3}$. To assess the loss of particles in the flow tube system, the size distribution of the aerosol flow in the absence of gaseous alkylamides was measured before and after the flow tube at < 3% and 80% RH, respectively, as shown in Supporting Information (SI) Figure S1. In both cases, the surface area-to-volume ratios of the aerosol flow were less than 5% variation. Particle loss within the flow tube system was negligible. As shown in Figure 1, another flow of pure air was used to keep the flow entering the flow tube constant throughout one experiment when the aerosol flow was bypassed from the aerosol flow tube.

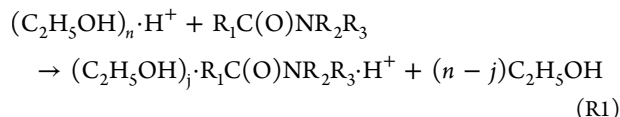
Gaseous alkylamides (C_1 to C_3) were generated using homemade permeation sources. FA ($\geq 99.5\%$, Sigma-Aldrich), AA ($\sim 99\%$, Sigma-Aldrich), *N*-methylformamide, (MF, 99%, Sigma-Aldrich), propanamide (PA, 97%, Sigma-Aldrich), *N*-methylacetamide (MA, $\geq 99\%$, Sigma-Aldrich), and DMF ($\geq 99\%$, Sigma-Aldrich) were used as received without further purification. The permeation tube was placed in a glass tube with an inner diameter of 2.5 cm that was immersed in a constant temperature liquid bath.²⁶ An ultrahigh purity (UHP) nitrogen ($\geq 99.999\%$, Pujiang Specialty Gases Factory, China) flow of typically 0.1 slpm was passed through the glass tube to entrain the corresponding alkylamide into the gas flow, and then directed into the aerosol flow tube through one side injector. In order to reduce the wall loss of gaseous alkylamides, a Teflon layer was coated on the inner wall of the aerosol flow tube and the outer wall of the stainless-steel injector.

The other side injector was retained for a pure air flow typically at 3.5 slpm. The total flow rate in the aerosol flow tube was approximately 6.3 slpm, corresponding to a Reynolds number of ~ 113 . Therefore, a laminar flow profile was assumed to have been established with a corresponding linear flow velocity around 2.0 cm/s during our experiments.

An aerodyne HRTof-CIMS that allows mass spectrometric measurements with high sensitivity and high mass resolution was used to monitor the concentrations of gaseous alkylamides during the uptake experiments. The instrumentation has been described in details in previous studies.^{16,27} In this work, we used protonated ethanol as reagent ions due to its higher proton affinity ($185.6 \text{ kcal mol}^{-1}$) compared to that of water ($165.2 \text{ kcal mol}^{-1}$)^{16,28–30} and therefore more selectivity for

detecting species whose proton affinities are even higher (e.g., $>196 \text{ kcal mol}^{-1}$ for alkylamides³¹).

Alkylamides were detected through the following ion–molecule reaction:



where $n = 1, 2, 3$; $j = 0, 1$; $\text{R}_1\text{C}(\text{O})\text{NR}_2\text{R}_3$ donates alkylamides; and $(\text{C}_2\text{H}_5\text{OH})_j \cdot \text{R}_1\text{C}(\text{O})\text{NR}_2\text{R}_3 \cdot \text{H}^+$ donates the protonated alkylamides and their clusters with ethanol. Concentrations of alkylamides were in the range of hundreds of pptv to a few ppbv, estimated using the calibration coefficients from a previous study.¹⁶ Note that the measured signal intensities for protonated alkylamides were then corrected by subtracting the instrumental background, which was generally less than 7% of the initial signal intensities of the alkylamides in all of our uptake experiments.

The chemical composition of sulfuric acid particles after exposure to FA or DMF was analyzed by HRTof-CIMS that was interfaced to a Filter Inlet for Gases and AEROSols (FIGAERO). Briefly, FIGAERO-HRTof-CIMS provides unperturbed measurements of gaseous samples while collecting particles on a PTFE filter via an entirely separate sampling port.³² Analysis of collected particles was conducted via evaporation from the filter using temperature-programmed thermal desorption by heated UHP N_2 . Note that, before filter collection, we specifically directed the aerosol sample flow through a cylindrical diffusion scrubber filled with activated charcoal to remove the redundant gaseous alkylamides. Particle loss in the scrubber was negligible. The typical collection time for the aerosol flow was 10 min.

Uptake of a gas-phase species by a liquid surface can be treated by a diffusional and reactional equation.³³ The observed first-order rate coefficient k_{obs} is derived from the observed decay in the absence and presence of sulfuric acid aerosols, as given in eq 1:

$$k_{\text{obs}} = \frac{u}{L} \ln \left(\frac{I_0}{I_t} \right) \quad (1)$$

where u is the carrier gas flow velocity (cm s^{-1}), L is the contact distance between the gaseous alkylamide and suspended sulfuric acid particles, I_0 is the initial signal intensity of the alkylamide and I_t is the signal intensity of the alkylamide after a reaction time of t (corresponding to a contact distance of L). The uptake coefficient γ is then determined using eq 2:

$$\gamma = \frac{4k_p}{S \cdot \omega_{\text{amide}}} \quad (2)$$

where $k_p = k_{\text{obs}} - k_w$ is the first-order rate coefficient for loss of alkylamides onto the suspended aerosol particles, S is the total aerosol surface area-to-volume ratio of the aerosol flow obtained with the SMPS, ω_{amide} is the average molecular speed of the alkylamide in the gas phase, and k_w is the first-order rate coefficient for alkylamides' loss to the flow tube wall that is determined in the same manner as k_{obs} but in the absence of particles. k_w is generally larger at higher RH, and a k_w of $< 0.0017 \text{ s}^{-1}$ for DMF was measured at 293 K and $\sim 80\%$ RH. The values of k_w were much smaller than those of k_p in the same experiment in this study. The extent of the uptake can be

varied by either changing the contact distance, or changing the aerosol surface area-to-volume ratio.

3. RESULTS AND DISCUSSION

Uptake Measurements. Alkylamide uptake experiments were performed by measuring the decay of the gaseous alkylamide. Figure 2 shows a typical profile of the decay in the

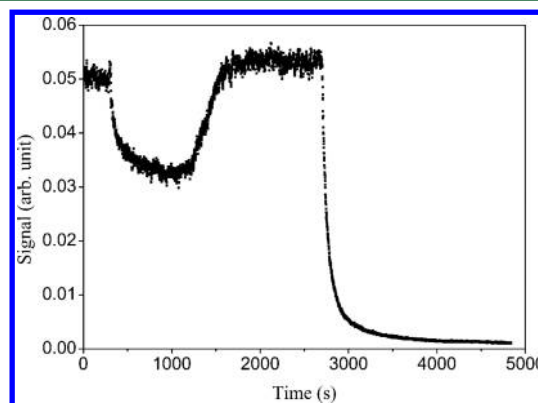


Figure 2. A typical temporal profile for the uptake of formamide (FA) by suspended sulfuric acid particles at $\text{RH} < 3\%$, $T = 293 \pm 1 \text{ K}$, and $L = 65 \text{ cm}$. Note that FA was bypassed at 2700 s.

alkylamide signal upon exposure to H_2SO_4 particles at 293 K and $< 3\%$ RH, using FA as an example. We first established a stable signal of FA with the aerosol flow being bypassed from the aerosol flow tube. Subsequently, as we introduced H_2SO_4 particles into the aerosol flow tube and exposed them to gaseous FA, a sharp decrease in the signal of FA was observed. When we bypassed H_2SO_4 particles again, the concentration of FA recovered to its original level, indicating that the uptake by suspended H_2SO_4 particles was responsible for the observed loss. FA was bypassed at 2700 s to establish an instrumental background for the gas phase FA. Analogous profiles were observed in all uptake experiments in this study.

Figure 3 plots the first-order rate coefficients k_p of FA (red triangles), MF (blue circles), and DMF (black squares) as a function of $(S \cdot \omega_{\text{amide}})/4$ under virtually identical experimental

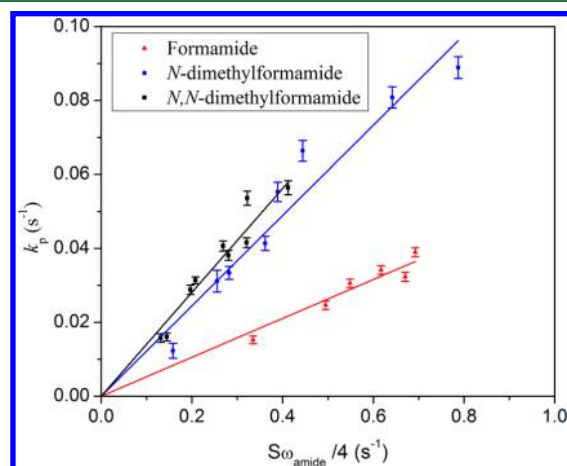
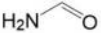
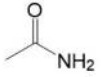
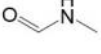
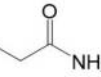
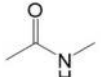
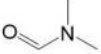


Figure 3. Plots of the first-order rate constant k_p as a function of $S \cdot \omega_{\text{amide}}/4$ at $\text{RH} < 3\%$, $T = 293 \pm 1 \text{ K}$, and $L = 65 \text{ cm}$. The slope for each fit represents the uptake coefficient γ as given by eq 2. The error bar represents one standard deviation.

Table 1. Summary of Uptake Coefficients

Compound	Molecular structure	Proton affinity (kcal mol ⁻¹)	RH (%)	T (K)	γ ($\times 10^{-2}$)
Formamide (FA)		196.5	< 3	293 ± 1	4.8 ± 0.1
Acetamide (AA)		206.4	< 3	338 ± 2 ^b	4.9 ± 0.6
			< 3	293	9.4 ^a
<i>N</i> -Methylformamide (MF)		203.5	< 3	293 ± 1	12 ± 1
			21 ± 2	293 ± 1	0.59 ± 0.24
			50 ± 2	293 ± 1	0.10 ± 0.12
Propanamide (PA)		209.4	< 3	338 ± 2 ^b	5.0 ± 0.6
			< 3	293	9.6 ^a
<i>N</i> -Methylacetamide (MA)		212.4	< 3	293 ± 1	23 ± 1
<i>N,N</i> -Dimethylformamide (DMF)		212.1	< 3	293 ± 1	14 ± 1
			< 3	315 ± 2 ^b	9.7 ± 0.7
			< 3	335 ± 2 ^b	8.2 ± 0.4
			< 3	355 ± 2 ^b	5.3 ± 0.2
			22 ± 2	293 ± 1	1.2 ± 0.1
			54 ± 2	293 ± 1	0.23 ± 0.09
			80 ± 2	293 ± 1	0.13 ± 0.08

^aEstimated values using the temperature-dependence for the uptake coefficients of DMF on suspended H₂SO₄ particles acquired in this study.

^bExperiments were performed with a heating tape wrapped around the flow tube to regulate the temperature with an uncertainty of ± 1 K. A temperature gradient from the glass surface to the center of the flow tube was observed. Hence, shown here are cross section-weighted temperatures.

conditions, that is, RH < 3% and $T = 293 \pm 1$ K. The error bar represents one standard deviation that is a result of measurement uncertainties. With a correction of wall losses, such plots should be straight lines through the origin. Excellent R^2 values were obtained, being 0.99, 0.98, and 0.99 for FA, MF, and DMF, respectively. As shown in eq 2, the linear regression of each data set in Figure 3 yields an uptake coefficient γ . Similar plots were obtained for all of our uptake experiments.

Table 1 summarizes our measured uptake coefficients of six different alkylamides (C₁ to C₃) over a range of RHs and temperatures. Uptake coefficients of FA, MF, MA, and DMF were measured to be $(4.8 \pm 0.1) \times 10^{-2}$, $(12 \pm 1) \times 10^{-2}$, $(23 \pm 1) \times 10^{-2}$, and $(14 \pm 1) \times 10^{-2}$, respectively, at 293 K and < 3% RH. Attempts to measure the uptake coefficients of AA and PA at the same temperature were unsuccessful due to their relatively low volatility.³⁴ To cope with this problem, we performed measurements of these two alkylamides at an elevated temperature (338 K) by heating the aerosol flow tube with a uniformly wrapped heating tape. The measured uptake coefficients were $(4.9 \pm 0.6) \times 10^{-2}$ for AA and $(5.0 \pm 0.6) \times 10^{-2}$ for PA, respectively. By assuming the same temperature dependence for the uptake coefficients of AA and PA as that for DMF that will be discussed in the next section, we derived uptake coefficients of 9.6×10^{-2} and 9.7×10^{-2} , respectively, for AA and PA at 293 K and < 3% RH (Table 1). The two calculated uptake coefficients and those acquired experimentally for the other four alkylamides generally coincide with the relative values of their proton affinities as listed in Table 1. On the other hand, the measured uptake coefficient for MA is higher than the estimated one for AA, indicating that the steric hindrance of the ethyl substituent in the AA molecules might counteract the proton affinity, since the specific structure of a

molecule could be directly related to its capacity to interact with a surface.

Uptake As a Function of Relative Humidity. The measured uptake coefficients on a logarithmic scale of MF and DMF by suspended H₂SO₄ particles at 293 K are plotted as a function of RH, as shown in Figure 4. Both MF and DMF exhibit a large negative humidity dependence, of which the former one is more remarkable. The MF uptake coefficient decreases from $(12 \pm 1) \times 10^{-2}$ to $(0.10 \pm 0.12) \times 10^{-2}$ between < 3% and 50% RH, whereas the uptake coefficient of

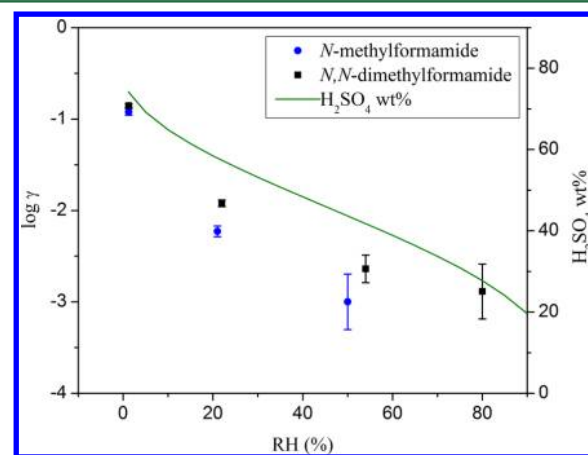


Figure 4. Uptake coefficient γ as a function of RH for *N*-methylformamide (MF) and *N,N*-dimethylformamide (DMF) at $T = 293 \pm 1$ K and $L = 65$ cm. The olive-green line is an estimation of H₂SO₄ concentration calculated using water vapor pressure data over aqueous sulfuric acid solution.^{41–44} The error bar represents one standard deviation.

DMF decreases from $(14 \pm 1) \times 10^{-2}$ to $(0.13 \pm 0.08) \times 10^{-2}$ between < 3% and 80% RH.

The overall uptake of gaseous molecules on aerosols is a sequence of coupled processes including accommodation, diffusion in the bulk phase involving either liquid or solid phases, and reaction in the bulk phase.^{35–37} Since a general solution of such equations cannot be obtained, an approximate equation based on a resistant model is used for expressing γ .^{38–40} In this study, the uptake coefficient for alkylamides upon sulfuric acid aerosols can be expressed as

$$\frac{1}{\gamma} = \frac{1}{\alpha} + \frac{1}{\Gamma_{\text{rxn}} + \Gamma_{\text{sol}}} \quad (3)$$

where α is mass accommodation coefficient, Γ_{sol} is the resistance due to solubility limitation, and Γ_{rxn} is the resistance due to reactions in the bulk phase. The terms on the right side of eq 3 represent the gas-to-particle transfer and the coupled reaction-diffusion processes in the bulk, respectively.

Within the relative humidity studied in this work, the concentration of sulfuric acid is in the range of 27–75 wt % H_2SO_4 , calculated using water vapor pressure data over aqueous sulfuric acid solution.^{41–44} In concentrated H_2SO_4 , the uptake of alkylamides is governed by mass accommodation,⁴⁵ since the rates of dissolution and reaction are faster than the mass accommodation. Previous studies on uptake of ammonia by H_2SO_4 solutions^{44,46} and uptake of alkylamines by H_2SO_4 solutions⁴⁷ also showed similar conclusions. Hence, the negative humidity dependence of the uptake coefficient γ is likely due to decreased mass accommodation coefficients α at lower acidities.^{44,46,47}

Uptake As a Function of Temperature. The temperature dependence of the multiphase uptake of DMF by suspended sulfuric acid particles has been investigated under RH < 3% and within a temperature range of 293–355 K. As shown in Table 1, the uptake coefficients of DMF by sulfuric acid particles decrease from $(14 \pm 1) \times 10^{-2}$ to $(5.3 \pm 0.2) \times 10^{-2}$ with the temperature increasing from 293 to 355 K, showing a negative dependence upon temperature.

As discussed in the previous section, the uptake of alkylamides by sulfuric acid particles under RH < 3% is governed by the mass accommodation coefficient. Hence, the temperature dependence of uptake coefficient γ here is in fact a temperature dependence of mass accommodation coefficient α . A thermodynamic model has been developed for the mass accommodation process based on the critical cluster theory.^{40,48} In this model, surface dynamics of the gas uptake process is viewed from the perspective of nucleation theory. The impinging gas-phase molecule (n_g) initially strikes the particle surface and becomes a loosely bound surface species (n_s) that participates in the nucleation process. If such a molecule becomes part of a critical sized cluster (n_s^*), it will serve as a center for further condensation and will grow/aggregate in size until it merges with the bulk phase. The temperature dependence of α is expressed in terms of an experimentally observed Gibbs free energy, ΔG_{obs} according to

$$\frac{\alpha}{1 - \alpha} = \frac{k_{\text{sol}}}{k_{\text{des}}} = \exp\left(\frac{-\Delta G_{\text{obs}}}{RT}\right) \quad (4)$$

where k_{des} is the rate of desorption from the surface, k_{sol} is the rate of transfer of molecules from the surface into the bulk phase, $\Delta G_{\text{obs}} = \Delta H_{\text{obs}} - T\Delta S_{\text{obs}}$ is the Gibbs free energy barrier of the transition state between the gaseous species (n_g) and the

critical cluster (n_s^*), and ΔH_{obs} and ΔS_{obs} represent the enthalpy and entropy changes during the accommodation, respectively.

In Figure 5, the natural log of $\gamma/(1-\gamma)$ is plotted as a function of $1/T$ using our uptake coefficients for DMF. It is

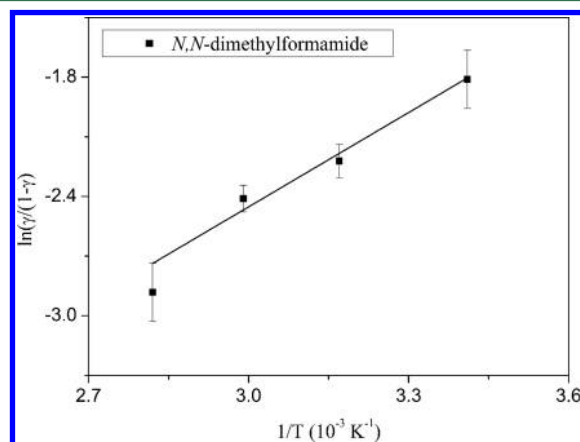


Figure 5. $\ln(\gamma/(1-\gamma))$ as a function of the reciprocal absolute temperature ($1/T$) for *N,N*-dimethylformamide (DMF) at RH < 3% and $L = 65$ cm. The slope of the fit represents $\Delta H/R$ and the intercept denotes $\Delta S/R$. The error bar represents one standard deviation.

evident from the plot that our data fit the model fairly well, indicating the observed temperature dependence is consistent with a mass accommodation-controlled multiphase uptake. $\Delta H_{\text{obs}}(\text{DMF}) = -(13.04 \pm 2.40) \text{ kJ}\cdot\text{mol}^{-1}$ and $\Delta S_{\text{obs}}(\text{DMF}) = -(57.57 \pm 7.46) \text{ J}\cdot\text{K}^{-1} \text{ mol}^{-1}$ are derived from the slope and the intercept of the plot, respectively. The values of ΔH_{obs} and ΔS_{obs} are always negative,^{40,48–50} reflecting that the mass accommodation process is always favored in terms of enthalpy, and that the dissolution of a trace gas into the aerosol corresponds to an entropy primarily contributed from the critical cluster binding energy and surface tension. The enthalpy and entropy changes for DMF in our study are smaller than those reported for NH_3 that were obtained from the uptake measurements in a droplet train flow reactor at pH 1, with $\Delta H_{\text{obs}}(\text{NH}_3) = -37.76 \text{ kJ}\cdot\text{mol}^{-1}$ and $\Delta S_{\text{obs}}(\text{NH}_3) = -150.27 \text{ J}\cdot\text{mol}^{-1} \text{ K}^{-1}$ (ref 46). From the critical cluster theory, the capacity of a gas molecule to participate in the aggregation process with solvent molecules defines the ease of the gas molecule's incorporation into bulk phase. This capacity is directly related to properties of both the solvent and the gas molecule, and in a way can be reflected by the magnitudes of the two parameters, ΔH_{obs} and ΔS_{obs} , that is, gas molecules with smaller ΔH_{obs} and ΔS_{obs} are more capable of forming a critical cluster.⁴⁰ Therefore, a higher solvent acidity in our study and a higher proton affinity of DMF ($212.1 \text{ kcal mol}^{-1}$)³¹ than that of NH_3 ($204.0 \text{ kcal mol}^{-1}$)³¹ can probably explain the observed difference in ΔH_{obs} and ΔS_{obs} between DMF and NH_3 . It is not surprising that alkylamides with higher proton affinities tend to have larger uptake coefficients, just as summarized previously in Table 1, since they are likely to be more actively bond to sulfuric acid molecules and easier to enter the bulk phase. On the other hand, care should be taken to extrapolate this dependence to the temperature outside the range and to other five alkylamides, although the critical cluster model fits the data set of DMF reasonably well.

Product Analysis. Here, we analyzed the chemical composition of sulfuric acid particles after exposure to FA or

DMF to elucidate the detailed reaction pathway within the particles. The experiments were performed under both wet and dry conditions, and by attaching a FIGAERO inlet to HRTof-CIMS.

Figure 6a depicts a typical temporal profile for experiments conducted under 50% RH. We first established a stable FA signal, and then introduced suspended H_2SO_4 particles into the

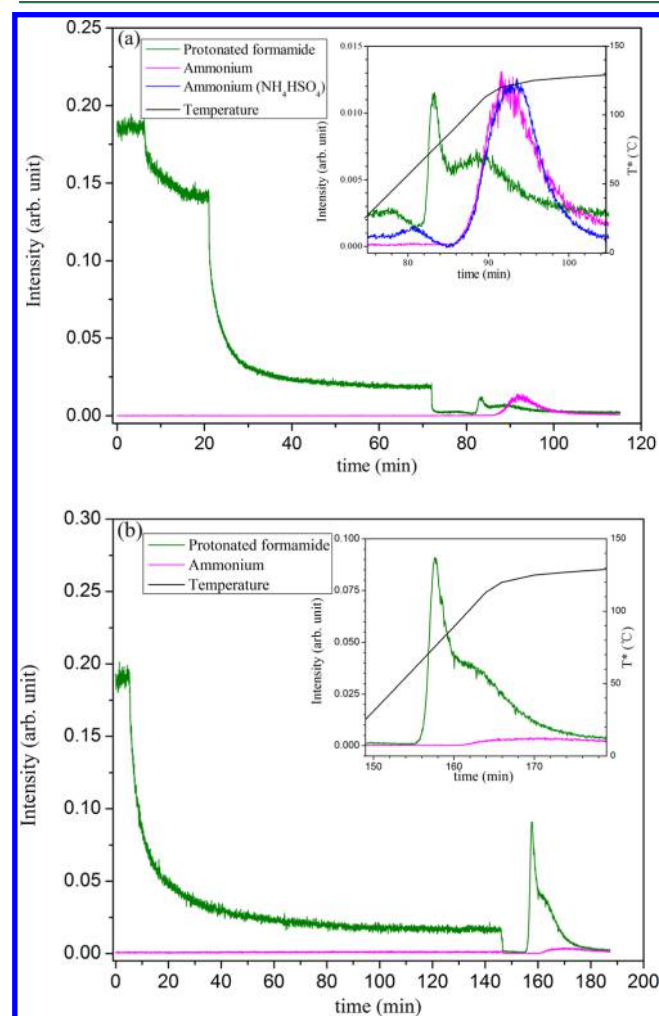


Figure 6. Typical temporal profiles for the chemical composition analysis of sulfuric acid particles after exposure to formamide (FA) under 50% RH (a) and < 3% RH (b). Take (a) for example: 0–6 min, establishment of a stable FA signal; 6–21 min, uptake of FA by suspended sulfuric acid particles under 50% RH; 21–72 min, the aerosol flow was directed through a denuder to remove the redundant FA, with a simultaneous particle collection between 62 and 72 min by the FIGAERO inlet; 72–115 min, chemical composition analysis of collected sulfuric acid particles using FIGAERO-HRTof-CIMS. On the top right is zoomed-in plots of protonated FA and ammonium during particle analysis, together with a plot of ammonium signal from an authentic NH_4HSO_4 solution analyzed by FIGAERO-HRTof-CIMS with the same thermal program. The asterisk denotes that the temperature was the reading from a temperature probe embedded in the FIGAERO inlet, not necessarily the true temperature for evaporation and decomposition. (b) is similar to (a) except that we directed the aerosol flow through the denuder to remove the redundant FA at the very beginning of the uptake experiment. Since the length of particle collection and the thermal program of particle analysis were both kept the same, the desorption process in (b) was identical to that in (a).

flow tube. Between 21 and 72 min, the aerosol flow was directed through a denuder to remove the redundant FA, with a simultaneous particle collection between 62 and 72 min by the FIGAERO inlet. The chemical composition of collected H_2SO_4 particles was analyzed using FIGAERO-HRTof-CIMS between 72 and 115 min.

Since protonated ethanol reagent ions were used, it is not surprising to observe the signal of protonated FA, which exhibits a double-peak thermogram in the plot. The first and narrower peak corresponds to FA molecules that strike the aerosol surface and becomes a loosely bound surface species (n_s) whereas the second peak at higher temperature corresponds to FA molecules that have been tightly interconnected and incorporated into the bulk liquid (n_b).⁴⁰ In addition, NH_4^+ was observed. The temporal profile of NH_4^+ from our collected H_2SO_4 particles coincided with that of NH_4^+ from an authentic NH_4HSO_4 solution analyzed by FIGAERO-HRTof-CIMS with the same thermal program (the blue line in the zoomed-in plots on the top right of Figure 6a), indicating the formation of ammonium salts during the uptake process. The results suggest that under 50% RH, the uptake of gaseous FA involves primarily two processes: the mass accommodation, and the hydrolysis of FA in the acidic particles followed by formation of ammonium.

As for experiments conducted under dry condition (Figure 6b), only two peaks of protonated FA were observed, and NH_4^+ was not found, indicating that hydrolysis of FA did not occur during the uptake under dry condition. This phenomena is consistent with previous findings that three water molecules are required to participate in the hydrolysis of one amide molecule.²⁵ Since there was hardly any water in suspended H_2SO_4 particles at < 3% RH, hydrolysis of FA would not tend to happen.

Analogically, hydrolysis of DMF was not observed for uptake experiments at < 3% RH, whereas $(\text{CH}_3)_2\text{H}_2\text{N}^+$, as a hydrolysis product from DMF according to the A_0T_2 mechanism, was identified at 90% RH uptake experiments.

4. ATMOSPHERIC IMPLICATIONS

Our measurements of the multiphase uptake of six alkylamides by suspended sulfuric acid particles allow us to assess the contribution of multiphase chemistry to the atmospheric loss processes of gaseous amides. Assuming a sulfuric acid aerosol population with a total surface area of $5 \times 10^2 \mu\text{m}^2 \text{cm}^{-3}$ and an average diameter of 100 nm that corresponds to $\sim 14 \mu\text{g m}^{-3}$ mass loading, the predicted lifetime of DMF with respect to multiphase loss on sulfuric acid aerosols at 298 K and 54% RH (~ 41 wt % H_2SO_4) is around 4 h. On the other hand, a 24 h daytime average global OH radical concentration of 10^6 molecules cm^{-3} (ref. 51) and a reported rate constant of $(1.4 \pm 0.3) \times 10^{-12} \text{cm}^3 \text{molecule}^{-1} \text{s}^{-1}$ for the OH radical-initiated reaction with DMF at 298 K¹⁸ leads to a lifetime of ~ 0.8 day for DMF. The lifetimes of DMF against NO_3 radicals and Cl atoms are 0.5 and 6 days,²⁰ respectively, using a 12h average nighttime NO_3 radical concentration of 5×10^8 molecules cm^{-3} (ref. 52) and an average global chlorine concentration of 10^4 molecules cm^{-3} (ref. 53). These estimates suggest that multiphase uptake of amides by acidic aerosols could be more competitive than gaseous oxidation in terms of atmospheric loss for DMF.

Furthermore, we have measured the uptake coefficients of MF and DMF by suspended sulfuric acid particles at 293 K and 58 wt % H_2SO_4 . Using the temperature dependence for DMF

obtained in our study, we derive that uptake coefficients of MF and DMF at 283 K are 0.71×10^{-2} and 1.4×10^{-2} , respectively. In a previous experimental study on uptake of three alkylamines (C_1 to C_3) by sulfuric acid at 283 K, uptake coefficients of $(2.0 \pm 0.2) \times 10^{-2}$, $(3.0 \pm 0.6) \times 10^{-2}$, and $(2.2 \pm 0.2) \times 10^{-2}$ were obtained for methylamine (by 62 wt % H_2SO_4), dimethylamine (by 62 wt % H_2SO_4), and trimethylamine (by 59 wt % H_2SO_4), respectively.⁴⁷ Clearly, under similar temperature and acidity, the estimated uptake coefficients for alkylamides here are smaller compared to those for alkylamines. Nevertheless, ambient concentrations of amides in urban Shanghai were reported to be at least an order of magnitude higher than those of amines.¹⁶ Hence, amides could compete with amines to react with acidic particles in places where concentrations of atmospheric amides are higher than those of amines. On the other hand, the water content of ambient acidic particles is presumably larger than that of the concentrated sulfuric acid particles used in our study, fulfilling the requirement for the presence of water in the particle. As a result, hydrolysis of amides is expected to occur with the formation of ammonium and aminium, adding more complexity to track particles' evolution.

■ ASSOCIATED CONTENT

📄 Supporting Information

The Supporting Information is available free of charge on the ACS Publications website at DOI: 10.1021/acs.est.7b03175.

Additional information regarding the surface area-weighted size distributions of sulfuric acid particles (PDF)

■ AUTHOR INFORMATION

Corresponding Author

*Phone: +86-21-65643568; e-mail: lin_wang@fudan.edu.cn.

ORCID

Mingyi Wang: 0000-0001-5782-2513

Lin Wang: 0000-0002-4905-3432

Present Address

§Center for Atmospheric Particle Studies, Carnegie Mellon University, Pittsburgh, Pennsylvania 15213, United States.

Notes

The authors declare no competing financial interest.

■ ACKNOWLEDGMENTS

This study was financially supported by the National Key R & D Program of China (2017YFC0209505), National Natural Science Foundation of China (No. 21222703, 21561130150, 41575113, and 91644213) and the Cyrus Tang Foundation (No. CTF-FD2014001). L.W. thanks the Royal Society-Newton Advanced Fellowship (NA140106).

■ REFERENCES

- (1) Cheng, Y.; Li, S. M.; Leithead, A. Chemical characteristics and origins of nitrogen-containing organic compounds in $PM_{2.5}$ aerosols in the Lower Fraser Valley. *Environ. Sci. Technol.* **2006**, *40*, 5846–5852.
- (2) Schmeltz, I.; Hoffmann, D. Nitrogen-containing compounds in tobacco and tobacco-smoke. *Chem. Rev.* **1977**, *77*, 295–311.
- (3) Ge, X. L.; Wexler, A. S.; Clegg, S. L. Atmospheric amines - Part I. A review. *Atmos. Environ.* **2011**, *45*, 524–546.
- (4) Leach, J.; Blanch, A.; Bianchi, A. C. Volatile organic compounds in an urban airborne environment adjacent to a municipal incinerator,

waste collection centre and sewage treatment plant. *Atmos. Environ.* **1999**, *33*, 4309–4325.

(5) El Dib, G.; Chakir, A. Temperature-dependence study of the gas-phase reactions of atmospheric NO_3 radicals with a series of amides. *Atmos. Environ.* **2007**, *41*, 5887–5896.

(6) Pitts, J. N.; Grosjean, D.; Vancauwenberghe, K.; Schmid, J. P.; Fitz, D. R. Photo-oxidation of aliphatic-amines under simulated atmospheric conditions - Formation of nitrosamines, nitramines, amides, and photo-chemical oxidant. *Environ. Sci. Technol.* **1978**, *12*, 946–953.

(7) Tuazon, E. C.; Atkinson, R.; Aschmann, S. M.; Arey, J. Kinetics and products of the gas-phase reactions of O_3 with amines and related-compounds. *Res. Chem. Intermed.* **1994**, *20*, 303–320.

(8) Malloy, Q. G. J.; Qi, L.; Warren, B.; Cocker, D. R., III; Erupe, M. E.; Silva, P. J. Secondary organic aerosol formation from primary aliphatic amines with NO_3 radical. *Atmos. Chem. Phys.* **2009**, *9*, 2051–2060.

(9) Murphy, S. M.; Sorooshian, A.; Kroll, J. H.; Ng, N. L.; Chhabra, P.; Tong, C.; Surratt, J. D.; Knipping, E.; Flagan, R. C.; Seinfeld, J. H. Secondary aerosol formation from atmospheric reactions of aliphatic amines. *Atmos. Chem. Phys.* **2007**, *7*, 2313–2337.

(10) Nielsen, C. J.; D'Anna, B.; Dye, C.; Graus, M.; Karl, M.; King, S.; Maguto, M. M.; Mueller, M.; Schmidbauer, N.; Stenstrom, Y.; Wisthaler, A.; Pedersen, S. Atmospheric chemistry of 2-aminoethanol (MEA). *Energy Procedia* **2011**, *4*, 2245–2252.

(11) Karl, M.; Dye, C.; Schmidbauer, N.; Wisthaler, A.; Mikoviny, T.; D'Anna, B.; Mueller, M.; Borrás, E.; Clemente, E.; Munoz, A.; Porras, R.; Rodenas, M.; Vazquez, M.; Brauers, T. Study of OH-initiated degradation of 2-aminoethanol. *Atmos. Chem. Phys.* **2012**, *12*, 1881–1901.

(12) Barsanti, K. C.; Pankow, J. F. Thermodynamics of the formation of atmospheric organic particulate matter by accretion reactions - Part 3: Carboxylic and dicarboxylic acids. *Atmos. Environ.* **2006**, *40*, 6676–6686.

(13) Zahardis, J.; Geddes, S.; Petrucci, G. A. The ozonolysis of primary aliphatic amines in fine particles. *Atmos. Chem. Phys.* **2008**, *8*, 1181–1194.

(14) Stockwell, C. E.; Jayarathne, T.; Cochrane, M. A.; Ryan, K. C.; Putra, E. I.; Saharjo, B. H.; Nurhayati, A. D.; Albar, I.; Blake, D. R.; Simpson, I. J.; Stone, E. A.; Yokelson, R. J. Field measurements of trace gases and aerosols emitted by peat fires in Central Kalimantan, Indonesia, during the 2015 El Niño. *Atmos. Chem. Phys.* **2016**, *16*, 11711–11732.

(15) Zhu, L.; Schade, G. W.; Nielsen, C. J. Real-time monitoring of emissions from monoethanolamine-based industrial scale carbon capture facilities. *Environ. Sci. Technol.* **2013**, *47*, 14306–14314.

(16) Yao, L.; Wang, M. Y.; Wang, X. K.; Liu, Y. J.; Chen, H. F.; Zheng, J.; Nie, W.; Ding, A. J.; Geng, F. H.; Wang, D. F.; Chen, J. M.; Worsnop, D. R.; Wang, L. Detection of atmospheric gaseous amines and amides by a High-Resolution Time-of-Flight Chemical Ionization Mass Spectrometer with protonated ethanol reagent ions. *Atmos. Chem. Phys.* **2016**, *16*, 14527–14543.

(17) Koch, R.; Palm, W. U.; Zetzsch, C. First rate constants for reactions of OH radicals with amides. *Int. J. Chem. Kinet.* **1997**, *29*, 81–87.

(18) Solignac, G.; Mellouki, A.; Le Bras, G.; Barnes, I.; Benter, T. Kinetics of the OH and Cl reactions with N-methylformamide, N,N-dimethylformamide and N,N-dimethylacetamide. *J. Photochem. Photobiol., A* **2005**, *176*, 136–142.

(19) Borduas, N.; da Silva, G.; Murphy, J. G.; Abbatt, J. P. D. Experimental and theoretical understanding of the gas phase oxidation of atmospheric amides with OH radicals: Kinetics, products, and mechanisms. *J. Phys. Chem. A* **2015**, *119*, 4298–4308.

(20) Barnes, I.; Solignac, G.; Mellouki, A.; Becker, K. H. Aspects of the atmospheric chemistry of amides. *ChemPhysChem* **2010**, *11*, 3844–3857.

(21) Roberts, J. M.; Veres, P. R.; Cochran, A. K.; Warneke, C.; Burling, I. R.; Yokelson, R. J.; Lerner, B.; Gilman, J. B.; Kuster, W. C.; Fall, R.; de Gouw, J. Isocyanic acid in the atmosphere and its possible

- link to smoke-related health effects. *Proc. Natl. Acad. Sci. U. S. A.* **2011**, *108*, 8966–8971.
- (22) Dahlin, J.; Spanne, M.; Karlsson, D.; Dalene, M.; Skarping, G. Size-separated sampling and analysis of isocyanates in workplace aerosols. Part I. Denuder-cascade impactor sampler. *Ann. Occur. Hyg.* **2008**, *52*, 361–374.
- (23) Glasoe, W. A.; Volz, K.; Panta, B.; Freshour, N.; Bachman, R.; Hanson, D. R.; McMurry, P. H.; Jen, C. Sulfuric acid nucleation: An experimental study of the effect of seven bases. *J. Geophys. Res. Atmos.* **2015**, *120*, 1933–1950.
- (24) Smith, C. R.; Yates, K. Medium and temperature dependence of acid-catalyzed hydrolysis of N-methylated methylbenzimidates and benzoylimidazole - investigation into mechanism of amide hydrolysis. *J. Am. Chem. Soc.* **1972**, *94*, 8811–8817.
- (25) Cox, R. A.; Yates, K. The hydrolyses of benzamides, methylbenzimidatium ions, and lactams in aqueous sulfuric-acid - the excess acidity method in the determination of reaction-mechanisms. *Can. J. Chem.* **1981**, *59*, 2853–2863.
- (26) Zheng, J.; Ma, Y.; Chen, M. D.; Zhang, Q.; Wang, L.; Khalizov, A. F.; Yao, L.; Wang, Z.; Wang, X.; Chen, L. X. Measurement of atmospheric amines and ammonia using the High Resolution Time-of-Flight Chemical Ionization Mass Spectrometry. *Atmos. Environ.* **2015**, *102*, 249–259.
- (27) Wang, M. Y.; Yao, L.; Zheng, J.; Wang, X. K.; Chen, J. M.; Yang, X.; Worsnop, D. R.; Donahue, N. M.; Wang, L. Reactions of atmospheric particulate stabilized criegee intermediates lead to high-molecular-weight aerosol components. *Environ. Sci. Technol.* **2016**, *50*, 5702–5710.
- (28) Nowak, J. B.; Huey, L. G.; Eisele, F. L.; Tanner, D. J.; Mauldin, R. L.; Cantrell, C.; Kosciuch, E.; Davis, D. D. Chemical ionization mass spectrometry technique for detection of dimethylsulfoxide and ammonia. *J. Geophys. Res.* **2002**, *107*, ACH 10–1–ACH 10–1.
- (29) You, Y.; Kanawade, V. P.; de Gouw, J. A.; Guenther, A. B.; Madronich, S.; Sierra-Hernandez, M. R.; Lawler, M.; Smith, J. N.; Takahama, S.; Ruggeri, G.; Koss, A.; Olson, K.; Baumann, K.; Weber, R. J.; Nenes, A.; Guo, H.; Edgerton, E. S.; Porcelli, L.; Brune, W. H.; Goldstein, A. H.; Lee, S. H. Atmospheric amines and ammonia measured with a chemical ionization mass spectrometer (CIMS). *Atmos. Chem. Phys.* **2014**, *14*, 12181–12194.
- (30) Yu, H.; Lee, S. H. Chemical ionisation mass spectrometry for the measurement of atmospheric amines. *Environ. Chem.* **2012**, *9*, 190–201.
- (31) NIST NIST Standard Reference Database Number 69, edited, National Institute for Standard Technology (NIST) Chemistry Web Book. <http://webbook.nist.gov/chemistry/> (accessed June 14, 2017).
- (32) Lopez-Hilfiker, F. D.; Mohr, C.; Ehn, M.; Rubach, F.; Kleist, E.; Wildt, J.; Mentel, T. F.; Lutz, A.; Hallquist, M.; Worsnop, D.; Thornton, J. A. A novel method for online analysis of gas and particle composition: Description and evaluation of a Filter Inlet for Gases and AEROSols (FIGAERO). *Atmos. Meas. Tech.* **2014**, *7*, 983–1001.
- (33) Ammann, M.; Cox, R. A.; Crowley, J. N.; Jenkin, M. E.; Mellouki, A.; Rossi, M. J.; Troe, J.; Wallington, T. J. Evaluated kinetic and photochemical data for atmospheric chemistry: Volume VI - heterogeneous reactions with liquid substrates. *Atmos. Chem. Phys.* **2013**, *13* (13), 8045–8228.
- (34) Bernauer, M.; Dohnal, V. Temperature dependence of air-water partitioning of N-Methylated (C1 and C2) fatty acid amides. *J. Chem. Eng. Data* **2008**, *53*, 2622–2631.
- (35) Akimoto, H. *Introduction to Atmospheric Chemistry*; Springer Japan: Japan, 2016; p 421.
- (36) Carslaw, K. S.; Peter, T.; Müller, R. Uncertainties in reactive uptake coefficients for solid stratospheric particles 0.2. Effect on ozone depletion. *Geophys. Res. Lett.* **1997**, *24*, 1747–1750.
- (37) Guimbaud, C.; Arens, F.; Gutzwiller, L.; Gaggeler, H. W.; Ammann, M. Uptake of HNO₃ to deliquescent sea-salt particles: a study using the short-lived radioactive isotope tracer N-13. *Atmos. Chem. Phys.* **2002**, *2*, 249–257.
- (38) Schwartz, S. E., Mass-transport considerations pertinent to aqueous phase reactions of gases in liquid-water clouds. In *Chemistry of Multiphase Atmospheric Systems*; Jaeschke, W., Ed.; Springer Berlin Heidelberg: Berlin, Heidelberg, 1986; pp 415–471.
- (39) Worsnop, D. R.; Zahniser, M. S.; Kolb, C. E.; Gardner, J. A.; Watson, L. R.; Vandoren, J. M.; Jayne, J. T.; Davidovits, P. Temperature-dependence of mass accommodation of SO₂ and H₂O₂ on aqueous surfaces. *J. Phys. Chem.* **1989**, *93*, 1159–1172.
- (40) Davidovits, P.; Kolb, C. E.; Williams, L. R.; Jayne, J. T.; Worsnop, D. R. Update 1 of: mass accommodation and chemical reactions at gas-liquid interfaces. *Chem. Rev.* **2011**, *111*, PR76–PR109.
- (41) Tang, I. N.; Munkelwitz, H. R. Water activities, densities, and refractive-indexes of aqueous sulfates and sodium-nitrate droplets of atmospheric importance. *J. Geophys. Res.* **1994**, *99*, 18801–18808.
- (42) Tang, I. N. Chemical and size effects of hygroscopic aerosols on light scattering coefficients. *J. Geophys. Res. Atmos.* **1996**, *101*, 19245–19250.
- (43) Perry, R. H.; Green, D. W.; Maloney, J. O. *Perry's Chemical Engineers' Handbook*, 7th ed.; McGraw-Hill: New York, 2007.
- (44) Swartz, E.; Shi, Q.; Davidovits, P.; Jayne, J. T.; Worsnop, D. R.; Kolb, C. E. Uptake of gas-phase ammonia. 2. Uptake by sulfuric acid surfaces. *J. Phys. Chem. A* **1999**, *103*, 8824–8833.
- (45) Zhang, R. Y.; Wooldridge, P. J.; Molina, M. J. Vapor pressure measurements for the H₂SO₄/HNO₃/H₂O and H₂SO₄/HCl/H₂O Systems: Incorporation of stratospheric acids into background sulfate aerosols. *J. Phys. Chem.* **1993**, *97*, 8541–8548.
- (46) Shi, Q.; Davidovits, P.; Jayne, J. T.; Worsnop, D. R.; Kolb, C. E. Uptake of gas-phase ammonia. 1. Uptake by aqueous surfaces as a function of pH. *J. Phys. Chem. A* **1999**, *103*, 8812–8823.
- (47) Wang, L.; Lal, V.; Khalizov, A. F.; Zhang, R. Y. Heterogeneous chemistry of alkylamines with sulfuric acid: Implications for atmospheric formation of alkylammonium sulfates. *Environ. Sci. Technol.* **2010**, *44*, 2461–2465.
- (48) Nathanson, G. M.; Davidovits, P.; Worsnop, D. R.; Kolb, C. E. Dynamics and kinetics at the gas-liquid interface. *J. Phys. Chem.* **1996**, *100*, 13007–13020.
- (49) Hallquist, M.; Stewart, D. J.; Baker, J.; Cox, R. A. Hydrolysis of N₂O₅ on submicron sulfuric acid aerosols. *J. Phys. Chem. A* **2000**, *104*, 3984–3990.
- (50) Griffiths, P. T.; Cox, R. A. Temperature dependence of heterogeneous uptake of N₂O₅ by ammonium sulfate aerosol. *Atmos. Sci. Lett.* **2009**, *10*, 159–163.
- (51) Hein, R.; Crutzen, P. J.; Heimann, M. An inverse modeling approach to investigate the global atmospheric methane cycle. *Global Biogeochem. Cycles* **1997**, *11*, 43–76.
- (52) Atkinson, R. Kinetics and mechanisms of the gas-phase reactions of the NO₃ radical with organic-compounds. *J. Phys. Chem. Ref. Data* **1991**, *20*, 459–507.
- (53) Wingenter, O. W.; Kubo, M. K.; Blake, N. J.; Smith, T. W.; Blake, D. R.; Rowland, F. S. Hydrocarbon and halocarbon measurements as photochemical and dynamical indicators of atmospheric hydroxyl, atomic chlorine, and vertical mixing obtained during Lagrangian flights. *J. Geophys. Res. Atmos.* **1996**, *101*, 4331–4340.